DOI 10.1007/978-1-4899-8005-2_13
Reprinted from *Solar Physics* Journal, DOI 10.1007/s11207-013-0345-1

A Comparison of Solar Cycle Variations in the Equatorial Rotation Rates of the Sun's Subsurface, Surface, Corona, and Sunspot Groups

J. Javaraiah

Received: 13 February 2012 / Accepted: 6 June 2013 / Published online: 18 July 2013

Abstract Using the *Solar Optical Observing Network* (SOON) sunspot-group data for the period 1985 – 2010, the variations in the annual mean equatorial-rotation rates of the sunspot groups are determined and compared with the known variations in the solar equatorial-rotation rates determined from the following data: i) the plasma rotation rates at $0.94R_\odot, 0.95R_\odot, \ldots, 1.0R_\odot$ measured by the *Global Oscillation Network Group* (GONG) during the period 1995 – 2010, ii) the data on the soft-X-ray corona determined from *Yohkoh*/SXT full-disk images for the years 1992 – 2001, iii) the data on small bright coronal structures (SBCS) that were traced in *Solar and Heliospheric Observatory* (SOHO)/EIT images during the period 1998 – 2006, and iv) the Mount Wilson Doppler-velocity measurements during the period 1986 – 2007. A large portion (up to $\approx 30^\circ$ latitude) of the mean differential-rotation profile of the sunspot groups lies between those of the internal differential-rotation rates at $0.94R_\odot$ and $0.98R_\odot$. The variation in the yearly mean equatorial-rotation rate of the sunspot groups seems to be lagging behind that of the equatorial-rotation rate determined from the GONG measurements by one to two years. The amplitude of the GONG measurements is very small. The solar-cycle variation in the equatorial-rotation rate of the solar corona closely matches that determined from the sunspot-group data. The variation in the equatorial-rotation rate determined from the Mount Wilson Doppler-velocity data closely resembles the corresponding variation in the equatorial-rotation rate determined from the sunspot-group data that included the values of the abnormal angular motions ($> |3^\circ|\,\mathrm{day}^{-1}$) of the sunspot groups. Implications of these results are pointed out.

Solar Dynamics and Magnetism from the Interior to the Atmosphere
Guest Editors: R. Komm, A. Kosovichev, D. Longcope, and N. Mansour

J. Javaraiah (✉)
Indian Institute of Astrophysics, Bengaluru 560 034, India
e-mail: jj@iiap.res.in

1. Introduction

Studies on the solar-cycle variations in the solar differential rotation and meridional flow are important for understanding the physical system that generates solar activity and the solar cycle (Babcock, 1961; Ulrich and Boyden, 2005; Dikpati and Gilman, 2006; Karak, 2010). The solar differential rotation is well studied; in addition to using Doppler-velocity measurements, the data on different solar magnetic tracers are employed (mainly the sunspots and the sunspot groups). The results derived from the sunspot and the sunspot-group data show variations in both the equatorial-rotation rate and the latitude gradient of the rotation on several timescales, including timescales close to the 11-year solar cycle (Javaraiah and Gokhale, 1995; Javaraiah and Komm, 1999; Javaraiah, Bertello, and Ulrich, 2005a; Javaraiah, Bertello, and Ulrich, 2005b; Javaraiah and Ulrich, 2006; Brajša, Ruždjak, and Wöhl, 2006). Recently, Javaraiah (2011) detected variations on timescales of a few days, including 9 and 30 – 40 day quasi-periodicities, in the coefficients of differential rotation determined from the Mount Wilson Doppler-velocity data during Solar Cycle 22. The $\approx$ 11-year period torsional oscillation detected by Howard and LaBonte (1980) in the Mount Wilson Doppler-velocity measurements is confirmed by helioseismic studies (*e.g.* Howe *et al.*, 2000; Antia, Basu, and Chitre, 2008)

Javaraiah and Komm (1999) studied the variations in the coefficients of the differential rotation determined from the sunspot-group data (1879 – 1976) and the Mount Wilson Doppler-velocity data (1962 – 1994). They found considerable differences between the periodicities (> two years) in the rotational coefficients derived from the Doppler-velocity and the sunspot-group data. Javaraiah *et al.* (2009) analyzed the data on the solar surface equatorial-rotation rate derived from the more accurate Mount Wilson Doppler-velocity data during the period 1986 – 2007 and confirmed the short-term periodicities found by Javaraiah and Komm (1999) in the data before the year 1996, but found no statistically significant variation after 1996. That is, there is a very large difference between the temporal variations of the equatorial-rotation rate during Solar Cycle 22 (*i.e.* before 1995) and Cycle 23. Hence, it has been suspected that the frequent changes in the instrumentation of the Mount Wilson spectrograph may have made the data before 1995 erroneous and responsible for the variations in the equatorial-rotation rate derived from these data. To verify this, here we compare the variations in the equatorial-rotation rates derived from different rotational data and with different techniques.

2. Data and Analysis

2.1. Methodology

The solar differential rotation can be determined from the full-disk Doppler-velocity data using the traditional polynomial expansion

$$\omega(\phi) = A + B\sin^2\phi + C\sin^4\phi, \tag{1}$$

and from sunspot data by using the first two terms of the expansion, *i.e.*

$$\omega(\phi) = A + B\sin^2\phi, \tag{2}$$

where $\omega(\phi)$ is the solar sidereal angular velocity at heliographic latitude ϕ, the coefficient A represents the equatorial-rotation rate, and B and C measure the latitudinal gradient

in the rotation rate, with B mainly representing low latitudes and C mainly higher latitudes.

The sidereal rotation rate [ω, in degrees day^{-1}] of a sunspot or sunspot group is computed as (Carrington, 1863; Godoli and Mazzucconi, 1979; Balthasar, Vázquez, and Wöhl, 1986)

$$\omega = \frac{\Delta L}{\Delta t} + 14.18, \tag{3}$$

or as (*e.g.* Howard, Gilman, and Gilman, 1984; Kambry and Nishikawa, 1990; Gupta, Sivaraman, and Howard, 1999; Brajša, Ruždjak, and Wöhl, 2006)

$$\omega = \frac{\Delta D_{\mathrm{CM}}}{\Delta t} + 0.9856, \tag{4}$$

where ΔL, ΔD_{CM}, and Δt are the differences between the heliographic longitudes [L], the central meridian distances [D_{CM}], and the observation times [t] of two consecutive days of observations of the sunspot or sunspot group, respectively, and the values 14.18° day^{-1} and 0.9856 are the Carrington rigid-body rotation rate and the correction factor corresponding to the Earth's rotation, respectively. The quantity $\frac{\Delta D_{\mathrm{CM}}}{\Delta t}$ represents the synodic rotation rate. Within the uncertainties, both these methods yield the same result (the latter gives a relatively low value for the rotation rate; see Kambry and Nishikawa, 1990). Javaraiah and co-authors have used Equation (3) in all of their earlier articles (*e.g.* Javaraiah and Gokhale, 1995, 1997a, 1997b; Javaraiah and Komm, 1999; Javaraiah, 2003a, 2005; Javaraiah, Bertello, and Ulrich, 2005a, 2005b; Javaraiah and Ulrich, 2006). (Details on the method of conversion of the synodic to sidereal rotation rate can be found in some of the above cited articles, *e.g.* Brajša, Ruždjak, and Wöhl, 2006 and references therein.)

The solar differential rotation can also be studied by binning the data into latitude intervals of reasonably small size, *i.e.* without using the above equations (see the references above). This subject is reviewed by a number of authors (*e.g.* Javaraiah and Gokhale, 2002 and references therein).

2.2. Sunspot Group Data

Here the Greenwich sunspot-group data during the period of May 1874 – December 1976 and the SOON sunspot-group data during 1977 – 2010 were used. These data were taken from the website solarcience.msfc.nasa.gov/greenwich.shtml and consist of t, ϕ, L, D_{CM}, *etc.* for each sunspot group on each day of its observation. By using Equation (3), the ω values were determined from the data corresponding to each pair of the consecutive days' observations of the sunspot groups during the period 1986 – 2009. Each year's data were fitted to Equation (2). The latitudinal dependencies on the mean rotation rate of the sunspot groups over the whole period 1977 – 2011 (whole SOON data set) were determined by averaging the daily values of the rotational velocities in two-degree (and five-degree) latitude intervals and also by fitting the whole-period daily data to Equation (2). The data in both the northern and southern hemispheres were combined. These calculations were also made for the Greenwich data during the period May 1874 – December 1976.

Since the rotation rates of tracers depend on the lifetimes, sizes, and age of the tracers, the latitudinal dependence in the initial rotation rates (the first two days' heliographic positions of the sunspot groups were used) of the sunspot groups was also studied by classifying the sunspot groups on the basis of their lifetimes: one to three days, four to five days, six to eight days, and longer than eight days. For this, the combined Greenwich and SOON data were used.

The sunspot-group data that correspond to $|D_{CM}| > 75^\circ$ on any day of the sunspot group lifetime were excluded. To study the initial rotation rates of the sunspot groups, the data during the entire lifetime of a sunspot group were eliminated on any one day for which $|D_{CM}| > 75^\circ$ to avoid ambiguity in the identification of the first two days in the lifetimes of the sunspot groups. Since the cutoff of D_{CM} was applied to both the eastern and western sides, the sunspot groups that emerged at the visible side of the Sun and after a certain number of days moved to the other side were not taken into account in the data sample of any of the aforementioned classes (Note: each disk passage of a recurring sunspot group was treated as an independent sunspot group). As in our previous articles, we excluded the data correspond to $> 2^\circ$ day^{-1} latitudinal motions, and $> 3^\circ$ day^{-1} longitudinal motions (*i.e. abnormal ω values*). Ward (1965, 1966) found that this precaution substantially reduces the uncertainties in the results (see Javaraiah and Gokhale, 1995). However, the abnormal values of ω may have some physical significance. For example, the abnormal rotation rates of sunspot groups may play some role in the productions of solar flares (Hiremath and Suryanarayana, 2003; Suryanarayana, 2010). Hence, most of the above calculations were made for both the cases, *i.e.* the sets of the sunspot-group data with and without the abnormal ω values were used.

2.3. Mount Wilson Doppler-Velocity Data

The daily values of the equatorial-rotation rate [A] derived from the Mount Wilson Doppler measurements during the period 3 December 1985 to 5 March 2007 are available (Javaraiah *et al.*, 2009). This period covers Solar Cycle 22 and most of Cycle 23. The data have been corrected for scattered-light (for details see Ulrich, 2001). Javaraiah *et al.* (2009) used these data after removing the very large spikes (*i.e.* $> 2\sigma$, where σ is the standard deviation of the original time series) and studied short-term variations in the corrected data. The time series has data gaps that vary in size, with a maximum gap of 49 days during Carrington-Rotation numbers 1560 – 1608. Therefore, the daily data were binned to one-year consecutive intervals, and the annual average values of the equatorial-rotation rate (average of the daily values of A over each year) were determined. In Figure 1 of Javaraiah *et al.* (2009) both the original and the corrected time series of the equatorial-rotation rate were shown. In the present analysis the corrected time series was used.

2.4. Data on Subsurface and Coronal Rotation Rates

The Sun's internal-rotation rates determined from the GONG data for 147 intervals of three GONG-months (a GONG-month is 36 days), which began on 7 May 1995 and ended on 31 October 2009, for $0.005R_\odot, 0.01R_\odot, 0.015R_\odot, \ldots, 0.995R_\odot, 1.0R_\odot$, and for latitudes $0, 2, 4, \ldots, 88$ degrees are available (Antia and Basu, 2010). Figure 1 shows variations in the equatorial-rotation rate [Ω_0, angular velocity at latitude $\phi = 0$] at $0.94R_\odot, 0.95R_\odot, \ldots, 1.0R_\odot$. As can be seen in this figure, the temporal patterns of the equatorial-rotation rates at the different depths are mostly similar. However, there is a suggestion that some features are smoothed when going from the interior toward the surface and *vice versa*. Specifically, the maxima in 2002 and 2008 are smoothed in deeper layers while the minimum in 2005 is smoothed from the interior toward the surface.

The annual mean values of the equatorial-rotation rate of the soft X-ray corona determined from the *Yohkoh*/SXT solar full-disk images for the period 1992 – 2001 were taken from Table 2 of Chandra, Vats, and Iyer (2010), and those determined from the rotation rates of small bright coronal structures (SBCS) that were traced in SOHO/EIT images during the period 1998 – 2006 were taken from Figure 1 of Jurdana-Šepić *et al.* (2011).

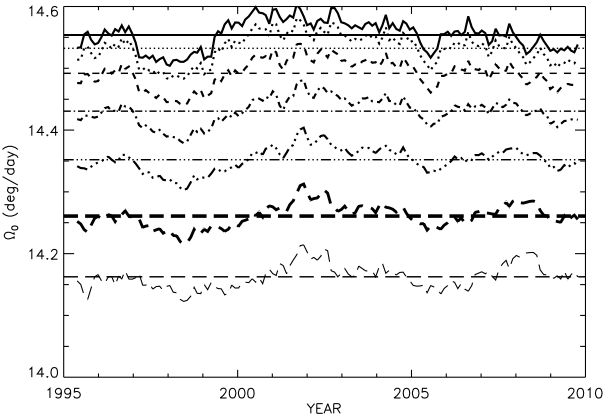

Figure 1 The solid, dotted, short-dashed, one dotted-dashed, three dotted-dashed, thick long-dashed, and thin long-dashed curves represent the variations in the equatorial-rotation rate [Ω_0] at $0.94R_\odot, 0.95R_\odot, \ldots, 1.0R_\odot$ (in the order of decreasing mean values of Ω_0), respectively, determined from the GONG data for 147 intervals of three GONG-months (for details about these data see Antia and Basu, 2010 and references therein).

3. Results

3.1. Depth Dependence in the Differential Rotation of Sunspot Groups

Figure 2 shows the latitudinal dependence on the mean rotation rate of sunspot groups determined from the SOON sunspot-group data during the period 1977 – 2011 separately from the data sets with and without the abnormal ω values. In the same figure the latitudinal dependencies on the mean (over the whole period 1995 – 2009) rotation rates of the plasma at different depths of the solar convection zone deduced from the GONG data are shown as well. As can be seen in this figure, a large portion (up to $\approx 30^\circ$ latitude) of the rotational profile that is obtained from the sunspot-group data that do not include the abnormal ω values lies between the corresponding profiles at $0.94R_\odot - 0.98R_\odot$ determined from the GONG data. Note that the value of the correlation coefficient shown in these figures is almost the same for any profile of the internal rotation shown in these figures. As can be seen in Figure 3, a similar conclusion can be drawn from the analysis of the large set of Greenwich data during May 1874 – December 1976 (however, the helioseismic measurements did not exist before 1995). The latitude dependence in the rotation determined from the sunspot-group data that included the abnormal ω values is obviously highly unrealistic. Since the equatorial-rotation rate determined from these data seems to be somewhat closer to the Ω_0 at $1.0R_\odot$, the comparison between its variation and that of the surface is studied here.

There are more abnormal values in the SOON (5.8 %) than in Greenwich data (2.9 %). In the Greenwich data the observation time contains the date with the fraction of a day. In the SOON data the fraction is rounded to 0.5 day. This might to some extent increase the number of abnormal ω values in the SOON data. Figure 4 shows the latitudinal dependence of the rotation determined by binning the sunspot-group data that included the abnormal ω values into five-degree latitude intervals. Obviously, the results show that the errors are much smaller than those shown in Figures 2(b) and 3(b). However, the latitudinal patterns of the data in five-degree latitude intervals (represented by the open circles) are mainly the same as the corresponding patterns of the data in the two-degree latitude intervals (*cf.* Figures 2(b) and 3(b)). The Greenwich data that included the abnormal ω values show rigid-body rotation (this is clearer in Figure 4(b) than in Figure 3(b)).

On average, the rotation rate determined from the magnetic tracers is higher than that derived from the Doppler-velocity measurements. This difference can be interpreted as the Doppler-velocity measurements representing the surface gas motion and the tracer motions

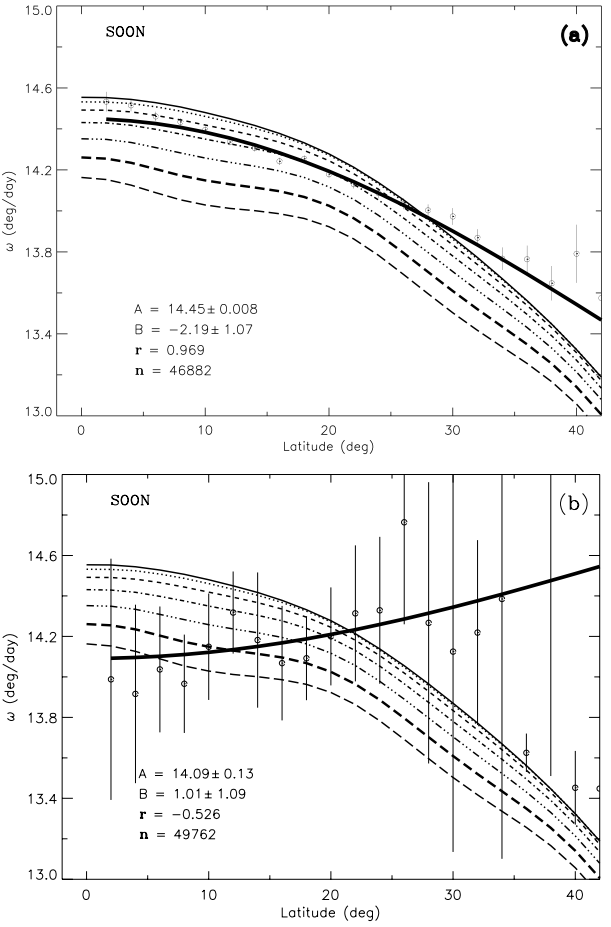

Figure 2 The latitudinal dependence of the mean rotation rates of sunspot groups determined by averaging the daily values of ω obtained from the SOON sunspot-group data during 1977 – 2011 over two-degree latitude intervals: $1° - 3°, 3° - 5°, 5° - 7°, \ldots, 40° - 42°$ (plotted at $2°, 4°, 6°, \ldots, 42°$). The error bars represent the standard errors. Panels (a) and (b) represent the data with and without the abnormal values of ω, respectively. The thick solid curve represents the corresponding mean profile deduced from the values (also shown) of the coefficients A and B of Equation (2) obtained from the total number of daily data [n]. The different curves represent the latitudinal dependencies on the mean (over the whole period 1995 – 2009) plasma rotation rates deduced from the GONG data at the same depths as in Figure 1. r represents the correlation coefficient between the sunspot group and the GONG data around $0.96R_{\odot}$ in $2°, 4°, 6°, \ldots, 36°$ latitudes.

representing the motions of the deeper layers (Foukal, 1972; Meunier, 2005), where the magnetic structures of the tracers are anchored. In addition to the concept of anchoring the magnetic structures of sunspot groups to the subsurface layers, the faster rotation rates of sunspots (faster than the photospheric plasma) have been explained in several ways: i) the emerging motion of the magnetic flux loop driven by buoyancy (*e.g.* Moreno-Insertis, 1986; Chou and Fisher, 1989; Shibata *et al.*, 1990), ii) geometrical projection effects (van Driel-Gesztelyi and Petrovay, 1990), iii) the drag due to ambient flows (Meyer *et al.*, 1979; Petrovay *et al.*, 1990), and iv) the interaction between magnetic buoyancy, drag, and Coriolis forces acting on the rising flux tubes (D'Silva and Howard, 1994). However, in spite of these effects, the similarity between the variation in the initial rotation rates of the sunspot groups with their lifetimes and the radial variation of the internal rotation rate determined from helioseismology suggests that the magnetic structures of sunspot groups with successively longer life times (2 – 12 days) are initially anchored in successively deeper layers of the Sun's convection zone (Javaraiah and Gokhale, 1997b). Hiremath (2002) confirmed this result by analyzing a large set of the Greenwich sunspot-group data, and Sivaraman *et al.* (2003) confirmed this by analyzing the sunspot-group data measured at the Mount Wilson and Kodaikanal Observatories. Short-lived and small sunspot groups predominate in a given

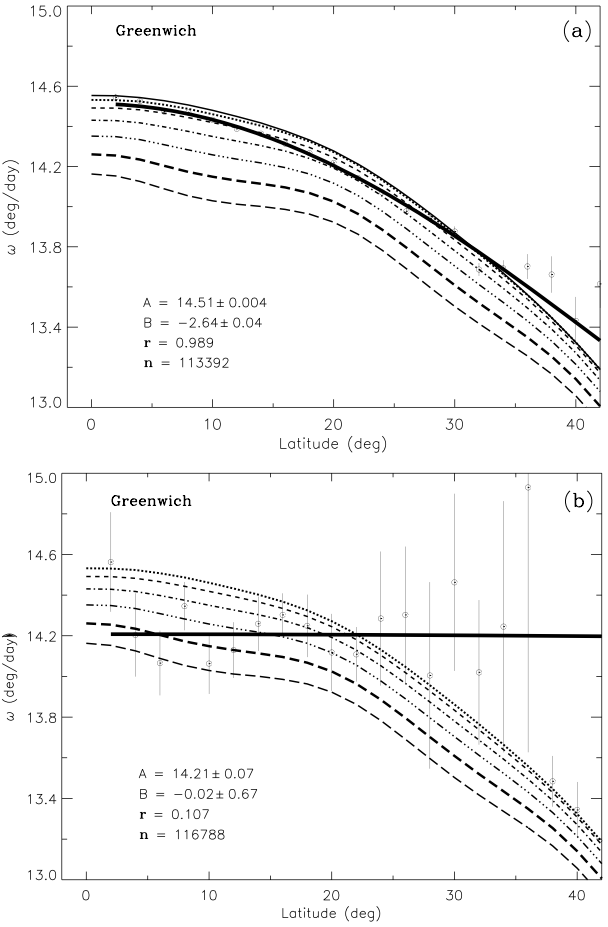

Figure 3 The latitudinal dependence of the mean rotation rates of sunspot groups determined by averaging the daily values of ω obtained from the Greenwich data during the period May 1874 – December 1976 over two-degree latitude intervals $1°-3°, 3°-5°, 5°-7°, \ldots, 40°-42°$ (plotted at $2°, 4°, 6°, \ldots, 42°$). The error bars represent the standard errors. Panels (a) and (b) represent the data with and without the abnormal values of ω, respectively. The thick solid curve represents the corresponding mean profile deduced from the values (also shown) of the coefficients A and B of Equation (2) obtained from the total number of daily data [n]. The different curves represent the latitudinal dependencies on the mean (over the whole period 1995 – 2009) plasma rotation rates deduced from the GONG data at the same depths as in Figure 1. r represents the coefficient of correlation between the sunspot group and the GONG data around $0.96R_\odot$ at $2°, 4°, 6°, \ldots, 36°$ latitude.

time interval (Javaraiah, 2012). Moreover, in the low latitudes near the base of the convection zone to near $0.8R_\odot$, the internal-rotation rate steeply increases and then gradually increases (or remains almost constant) up to near $0.95R_\odot$. The magnetic structures of the sunspot groups whose lifetimes exceed eight days seem to initially anchor in the layers below $0.8R_\odot$, and those of the sunspot groups with lifetimes of up to eight days seem to initially anchor in the layers above $0.8R_\odot$, as suggested by the pattern of the variation in the initial rotation rates of the sunspot groups with their lifetimes (see Javaraiah and Gokhale, 1997b). In Figure 5 the latitudinal dependencies on the mean initial rotation rates of the four different classes of sunspot groups whose lifetimes are in the ranges one to three, four to five, six to eight, and longer than eight days are compared with the latitudinal dependencies in the internal-rotation rates at depths $0.75R_\odot, 0.8R_\odot, 0.85R_\odot, 0.9R_\odot, 0.95R_\odot$, and $1.0R_\odot$. As can be seen in this figure, the portions up to 25° latitude in the profiles of the mean initial rotation rates of the shorter than and longer than eight days living sunspot groups are somewhat closer to those of the internal rotation at $0.94R_\odot - 0.96R_\odot$ and $0.8R_\odot$, respectively. These results are in general consistent with the results/suggestions in Javaraiah and Gokhale (1997b). The profile of the very short-lived sunspot groups is even higher than the rotation profile at $0.94R_\odot$. The angular motions of super-granules may influence the rotation rates of the very short-

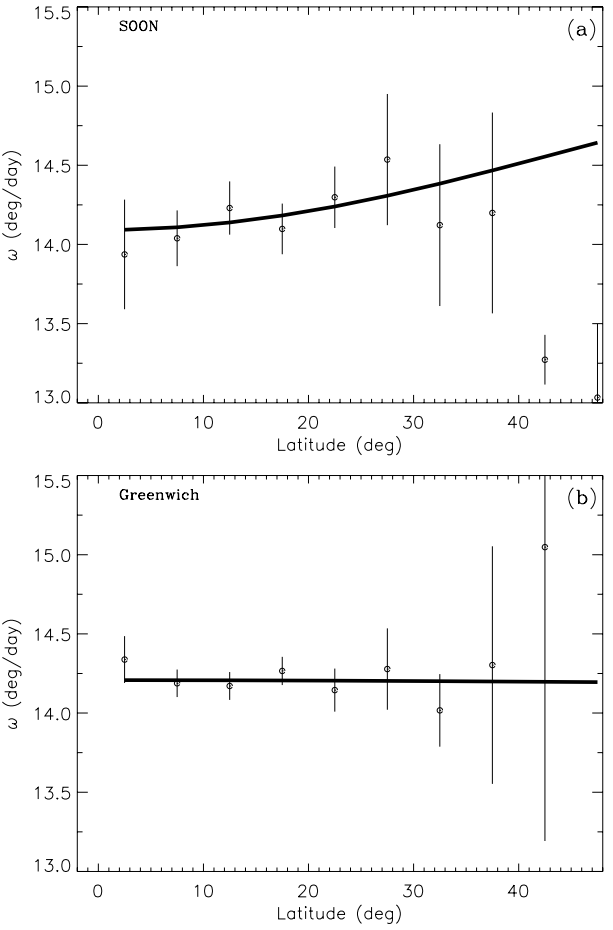

Figure 4 The latitudinal dependence of the mean rotation rates of sunspot groups determined by averaging the daily values of ω, obtained from the SOON (1977 – 2011) and Greenwich (1874 – 1976) sunspot-group data that included the abnormal values of ω, over five-degree latitude intervals, $0° – 5°$, $5° – 10°$, $10° – 15°$, ..., $45° – 50°$ (plotted at 2.5°, 7.5°, 12.5°, ..., 47.5°). The error bars represent the standard errors. The thick solid curve represents the corresponding mean profile deduced from the values of the coefficients A and B of Equation (2) obtained from the total number of daily data (*i.e.* the corresponding values that are given in Figures 2(b) and 3(b)).

lived sunspot groups. In this context it may be worth noting that the magnetohydrodynamic drag force may be strong on the small magnetic structures (D'Silva and Howard, 1994). The results (the profiles of the mean rotation rates of sunspot groups) shown in Figures 2 and 3 are determined from the combined data of all sunspot groups during all days in their respective lifetimes. These results as well as the results (the mean profiles of the initial rotation rates of sunspot groups) shown in Figures 5(a – c) are similar to the results found in most of the previous studies in which the sunspot groups were not sorted according to their lifetimes (Tuominen, 1962; Tuominen and Virtanen, 1988). Ruždjak *et al.* (2004) found that the initial velocity of recurring sunspot groups is higher than that of non-recurring sunspot groups and suggested that the recurring sunspot groups initially anchor at $0.93R_{\odot}$.

The range of the internal-rotation rate that corresponds to the increase in depth from $0.94R_{\odot} – 0.75R_{\odot}$ is approximately the same as that corresponding to the decrease in depth from $0.94R_{\odot} – 1.0R_{\odot}$. In view of the result that the magnetic structures of the sunspot groups with successively longer lifetimes (2 – 12 days) are initially anchored in successively deeper layers throughout the Sun's convection zone (Javaraiah and Gokhale, 1997b), in Figure 5 the internal-rotation rates are shown for a wide range of depths. In Figures 2 and 3 the mean rotation rates of the sunspot groups are compared with the internal-rotation rates at

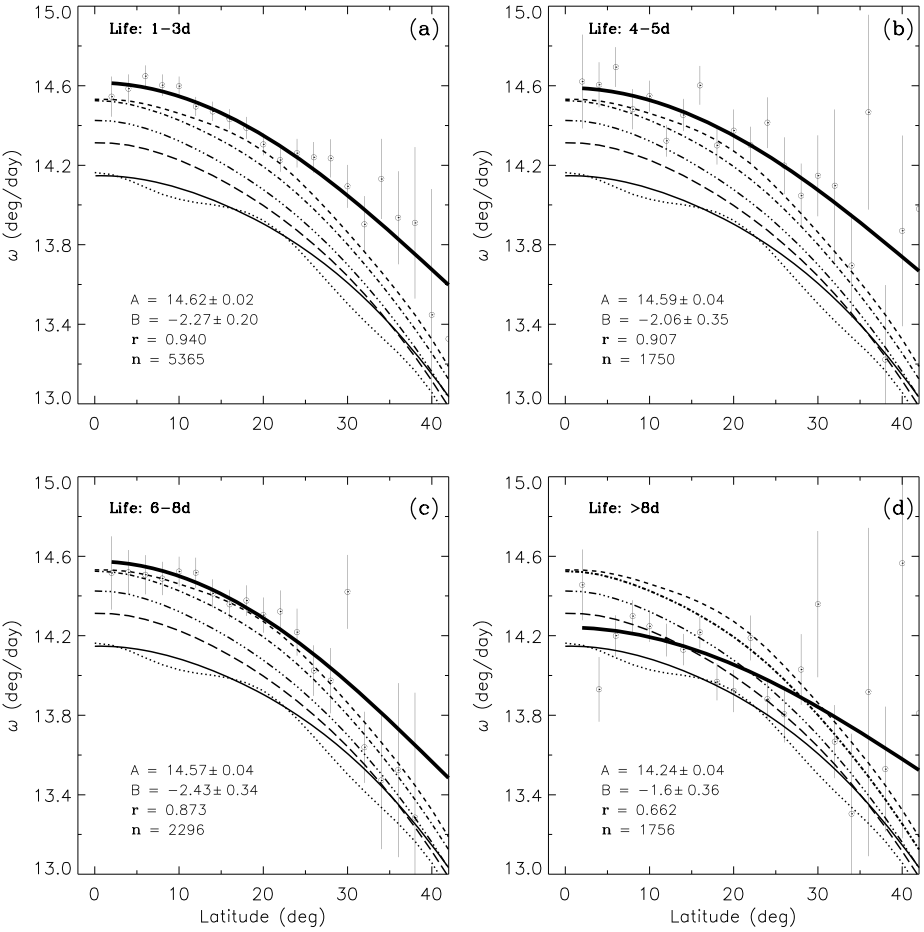

Figure 5 The latitudinal dependence of the mean initial rotation rates of sunspot groups whose life times are in the ranges (a) one to three days, (b) four to five days, (c) six to eight days, and (d) longer than eight days, determined from the combined Greenwich and SOON data during the period May 1874 – December 2011 by averaging the first-day values of ω over two-degree latitude intervals, $1^\circ - 3^\circ, 3^\circ - 5^\circ, 5^\circ - 7^\circ, \ldots, 40^\circ - 42^\circ$ (plotted at $2^\circ, 4^\circ, 6^\circ, \ldots, 42^\circ$). The error bars represent the standard errors. The thick solid curve represents the corresponding mean profile deduced from the values (also shown) of the coefficients A and B of Equation (2) obtained from the total number of daily data [n]. Here the internal-rotational profiles correspond to the different depths: thin-solid, long-dashed, three-dotted-dashed, one-dotted-dashed, dashed, and dotted curves represent the profiles at depths $0.75R_\odot$, $0.80R_\odot$, $0.85R_\odot$, $0.90R_\odot$, $0.95R_\odot$, and $1.0R_\odot$, respectively (sunspot-group data corresponding to $|D_{\rm CM}| \leq 75^\circ$ were used).

a narrow and somewhat shallower region, because the average rotation profile of sunspot groups is mostly contributed by the rotation rates of long-lived (lifetime longer than eight days) sunspot groups during the last few days of their lifetimes (Ruždjak *et al.*, 2004). The rotation rates of the long-lived and large sunspot groups are considerably lower during the initial and final days of their lifetimes.

The derived mean rotation rate of sunspot groups depends to some extent on the cutoff of $D_{\rm CM}$. It decreases for higher $D_{\rm CM}$ values (Ruždjak *et al.*, 2004 and references therein). In all their studies, Javaraiah and co-authors allowed $|D_{\rm CM}| \leq 75^\circ$. Ward (1965, 1966) allowed

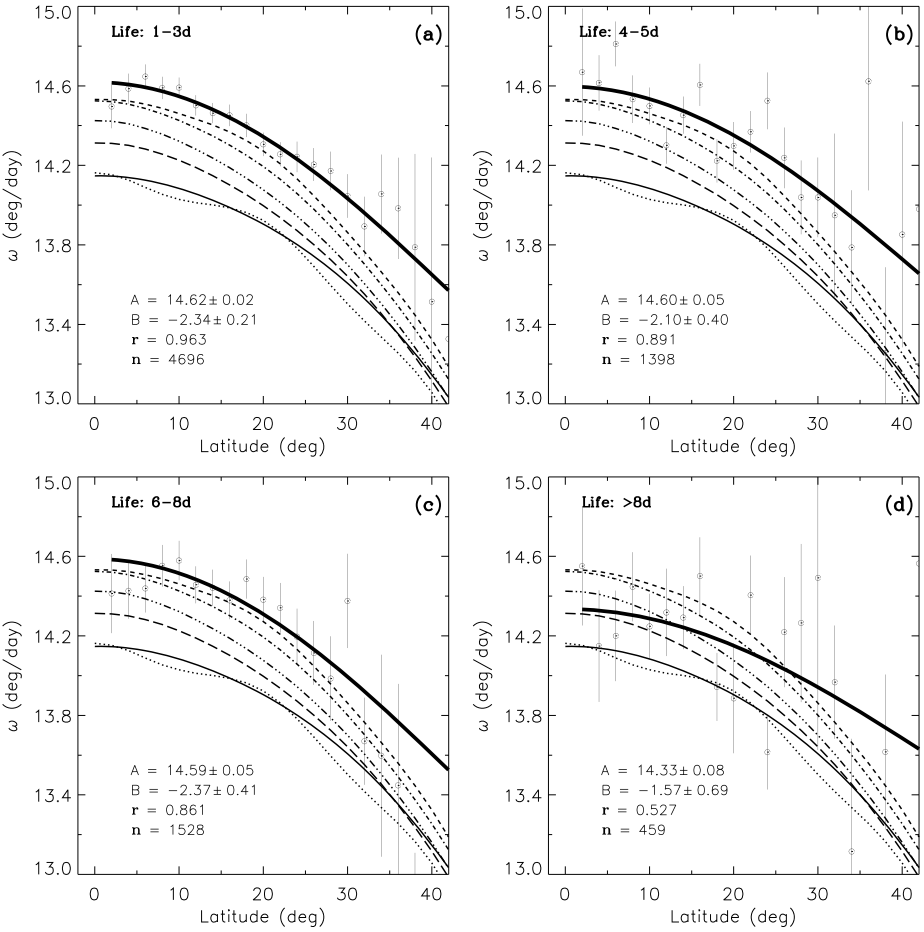

Figure 6 The same as Figure 5, but for the sunspot-group data corresponding to $|D_{\rm CM}| \leq 70^{\circ}$.

$|D_{\rm CM}|$ up to 80°, whereas many others allowed it up to $60^{\circ}-70^{\circ}$ only. A higher cutoff of $D_{\rm CM}$ reduces the contributions of long-lived sunspot groups somewhat, particularly contributions made during their initial and final days, for the derived mean rotation rate. Hence, the derived value of the mean rotation rate of sunspot groups is relatively high. However, it is necessary to verify that the first-day data sample is not contaminated with the sunspot groups arriving from other side of the Sun. To do this, we recalculated the results shown in Figure 5 by restricting $D_{\rm CM}$ up to $\pm 70^{\circ}$ only; the results are shown in Figures 6 and 7. These results are generally the same as those shown in Figure 5. Hence, the conclusions and inferences drawn above from the results shown in Figure 5 also hold for the results shown in Figures 6 and 7.

It is widely believed that magnetic flux, in the form of large flux tubes, emerges at the surface presumably from near the base of the convection zone (where the dynamo process is believed to be taking place) and is responsible for sunspots and other solar activity phenomena (see Rosner and Weiss, 1992; Gough, 2010). There are also suggestions and arguments that the sunspots form immediately beneath the surface (Kosovichev, Duvall, and

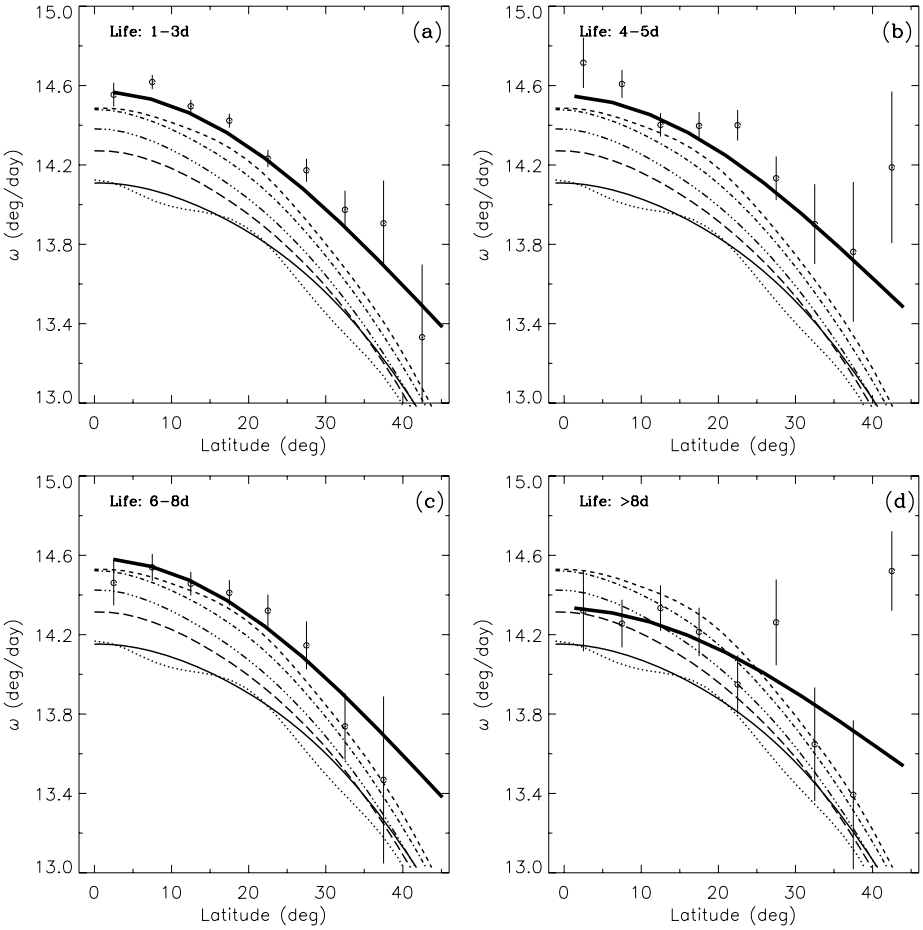

Figure 7 The latitudinal dependence of the mean initial rotation rates of sunspot groups whose life times are in the ranges of (a) one to three days, (b) four to five days, (c) six to eight days, and (d) longer than eight days, determined from the combined Greenwich and SOON data during the period May 1874 – December 2011 by averaging the first-day values of ω over five-degree latitude intervals, $0°-5°, 5°-10°, 10°-15°, \ldots, 45°-45°$ (plotted at $2.5°, 7.5°, 12.5°, \ldots, 47.5°$). The error bars represent the standard errors. Here the internal-rotational profiles correspond to the different depths: thin-solid, long–dashed, three-dotted-dashed, one-dotted-dashed, dashed, and dotted curves represent the profiles at depths $0.75R_\odot, 0.80R_\odot, 0.85R_\odot, 0.90R_\odot, 0.95R_\odot$, and $1.0R_\odot$, respectively. The sunspot-group data corresponding to $|D_{CM}| \leq 70°$ were used. The thick solid curve represents the corresponding mean profile deduced from the values of the coefficients A and B of Equation (2) obtained from the total number of daily data (*i.e.* the corresponding values that are given in Figure 6).

Scherrer, 2000; Kosovichev, 2002) and in different layers throughout the convection zone (Brandenburg, 2005). The results above are in general consistent with these suggestions and arguments, but they also support the idea that large magnetic structures might be generated near the base of the solar convection zone; many of the large magnetic structures may be fragmenting or branching into smaller structures while buoyantly rising through the solar convection zone, *i.e.* small magnetic structures may be fragmented or branched parts of the large magnetic structures (Javaraiah, 2003b). Schüssler and Rempel (2005) argued that the

dynamical disconnection of sunspots from their magnetic roots probably takes place during the final phases of their magnetic structures' buoyant ascent toward the surface.

3.2. Variation in the Equatorial-Rotation Rate

Figure 8 shows the variations in the annual mean values of the equatorial-rotation rate determined from the Doppler-velocity data and the sunspot-group data that did not include the abnormal values of ω. In this figure we also show the variations of the equatorial-rotation rates at $0.96R_\odot$ and $1.0R_\odot$ determined from GONG data for each of 147 intervals of three GONG-months during 1995 – 2009, the variation in the equatorial-rotation rate of the soft X-ray corona determined from the *Yohkoh*/SXT solar full-disk images for the period 1992 – 2001 and from the rotation rates of SBCS traced in SOHO/EIT images during the period 1998 – 2006 (Jurdana-Šepić *et al.*, 2011), and the annual mean sunspot number (Figure 8(b)) to study solar-cycle behavior of the equatorial-rotation rate. Since the mean value ($\approx 14.5^\circ$ day^{-1}) of the equatorial-rotation rate determined from the sunspot-group data during the period 1985 – 2010 is close to the mean Ω_0 at $0.96R_\odot$ (*cf.* Figures 2 and 3), the variation in the former is compared with that of the latter in addition to comparing it with the variation at $1.0R_\odot$ (due to the scaling problem the variation in Ω_0 at $1.0R_\odot$ is shown in Figure 8(a) instead of in Figure 8(b)). However, as can be seen in Figure 1, the patterns of the variations of the equatorial rotation rates at different depths are largely similar.

As can be seen in Figure 8, the mean value of the equatorial-rotation rate determined from the sunspot-group data is substantially higher (although it is lower during Cycle 22 than in the last 11 solar cycles (Javaraiah, Bertello, and Ulrich, 2005b; Suzuki, 2012)), and the amplitude of its variation is also about ten times higher than that determined from the Doppler-velocity measurements. The variation in the equatorial-rotation rate determined from the sunspot-group data steeply decreased during the rising phase of the Solar Cycle 22. It attained minimum at the maximum of this cycle and remained at approximately the same level up to the end of the cycle, then it steeply increased in the beginning of Cycle 23. The overall pattern suggests that there exists a quasi-11-year cycle in the equatorial-rotation rate (correlation coefficient ≈ -0.4, between sunspot number and A). At the beginning of Cycle 24 the equatorial-rotation rate is considerably higher than it was during the last about twenty years (including the beginnings of Cycles 22 and 23). The variation pattern in the equatorial-rotation rate is consistent with the well-known result of a higher rotation rate during the cycle minimum than during the maximum, which has been found in many studies (*e.g.* Brajša, Ruždjak, and Wöhl, 2006). However, it should be noted that the minimum years of the solar cycles contain mainly small sunspot groups (Javaraiah, 2012). These rotate faster than large sunspot groups (*e.g.* Howard, Gilman, and Gilman, 1984; Javaraiah and Gokhale, 1997b, see also Section 3.1 above). This property of the sunspot groups most probably has an influence on the aforementioned pattern of the solar cycle variation in the surface equatorial-rotation rate determined from the sunspot-group data.

The increases of rotational velocities in 2001 – 2002 and 2008 – 2009 are most pronounced in GONG results at $1.0R_\odot$. Similar increases also exist in the result obtained by using sunspot-group data (see Figure 8(a)). In fact, there is a reasonable agreement between the pattern of the variations in the equatorial-rotation rates determined from the sunspot-group data and the GONG data [Ω_0]. However, there is a considerable difference in the positions of the minima of these variations, giving the impression that the internal equatorial-rotation rate leads the equatorial-rotation rate of the sunspot groups by one to two years (the reason for this is not known to us).

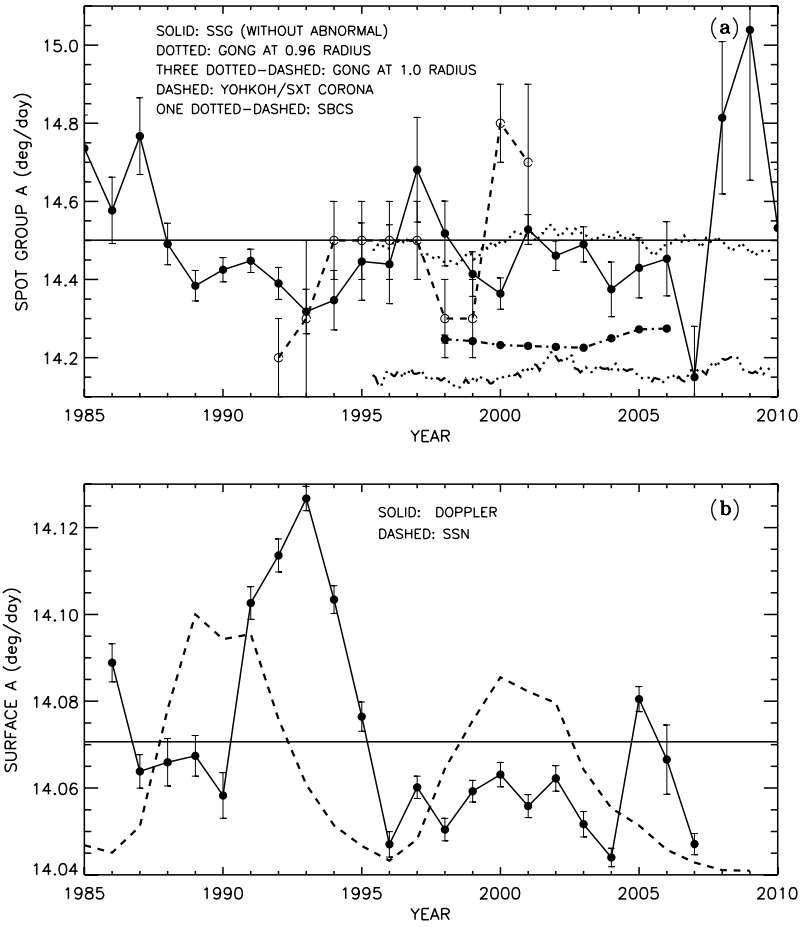

Figure 8 (a) Filled circle-solid curve: the variation in the annual equatorial-rotation rate A determined from the sunspot group (SSG) data after excluding the abnormal values of ω, which were calculated by using Equation (1). Open circle-dashed curve: the variations in the equatorial-rotation rate of the soft X-ray corona determined from *Yohkoh*/SXT full-disk images for the years 1992 – 2001 by Chandra, Vats, and Iyer (2010). Filled circle-one dotted-dashed curve: the variation in the annual mean equatorial-rotation rate determined from the data of SBCS, which were traced in SOHO/EIT images during the period 1998 – 2006 (Jurdana-Šepić *et al.*, 2011). In each of these cases the error-bars represent the values of 1σ obtained from the linear least-squares fits of the data (for SBCS σ has very low values). The dotted and three dotted-dashed curves are the variations in the equatorial-rotation rates at $0.96R_{\odot}$ and $1.0R_{\odot}$, determined from GONG data for each of the 147 intervals of the three GONG-months during 1995 – 2009 (Antia and Basu, 2010). The solid horizontal line is drawn at the mean values of $14.5° \pm 0.2°$ day^{-1}, determined from the yearly values of the sunspot-group data. (b) The solid curve represents the variation in the annual mean A determined from the corrected Mount Wilson Doppler-velocity data (Javaraiah *et al.*, 2009). The error bars represent one standard error (σ has very high values). The dashed curve represents the variation in the annual mean international sunspot number (SSN), which is normalized to the scale of A. The solid horizontal line is drawn at the mean value of A, $14.07° \pm 0.02°$ day^{-1}, determined from the yearly values. The Mount Wilson Doppler-velocity data in 2007 are available only up to March.

The annual variation in the equatorial-rotation rate determined from the Doppler-velocity data also steeply decreased during the rising phase and attained minimum at the sunspot maximum of Solar Cycle 22, but it increased sharply from 1990 to 1993 and suddenly

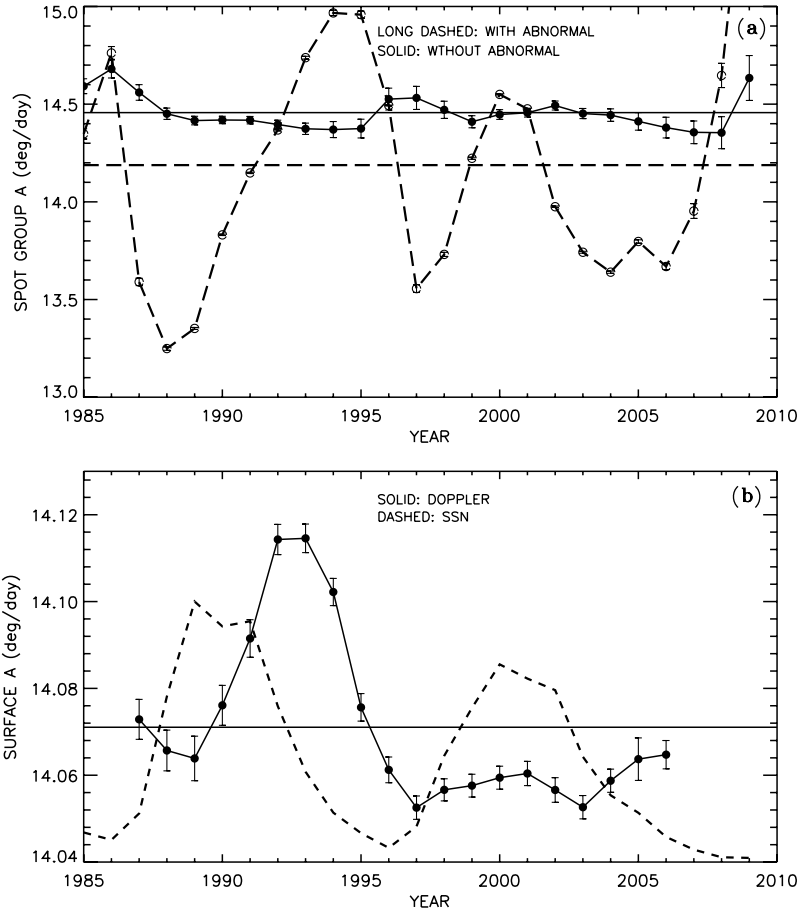

Figure 9 (a) The open circle-long-dashed and the filled circle-solid curves represent the variations in A derived from the sunspot group (SSG) data with and without abnormal ω values ($> 3^\circ$ day^{-1}), respectively, in three-year MTIs successively shifted by one year. In the first case the error-bars represent the standard error (because of the high σ value) and in the other case they represent the values of 1σ. The solid and long-dashed horizontal lines are drawn at the corresponding mean values of A, $14.46^\circ \pm 0.09^\circ$ day^{-1} and $14.19^\circ \pm 0.61^\circ$ day^{-1}. (b) The solid curve represents the three-year smoothed A derived from the annual mean values of A (shown in Figure 8(b)) determined from the Mount Wilson Doppler-velocity data (error bars represent one standard error). The solid horizontal line is drawn at the corresponding mean value of A, 14.07° day^{-1}. The dashed curve represents the variation in the annual mean international sunspot number (SSN), which is normalized to the scale of A. The Mount Wilson Doppler-velocity data in 2007 are available only up to March.

dropped from 1993 to 1994. Overall, the equatorial-rotation ration rate is low during Cycle 23, but there is an indication that the variation in the equatorial-rotation rate is in phase with the sunspot number in the interval 1998 – 2004 (however, the value of A suddenly increased around 2005 and then decreased). This behavior is opposite to that in the previous cycle. The overall pattern of the annual variation indicates that there is a five- to six-year periodicity in the equatorial-rotation rate during Cycle 22.

In Figure 9 we compare the variations in the equatorial-rotation rate determined from the Doppler-velocity data and the sunspot-group data that included the abnormal values of ω (*i.e.* $|\omega| > 3^\circ\,\mathrm{day}^{-1}$) calculated by using Equation (3). As already mentioned above, including the abnormal values of ω increases the uncertainties of the derived coefficients A and B, although the size of the data increased by 4 % – 5 % (the highest is 8.4 % around 2009). Hence, with the abnormal ω values the errors [σ] of the individual yearly averages are so large that they are not significantly (statistically) different from each other, so that the variations cannot be examined using them. Therefore, the values of A determined by binning the data into three-year moving time intervals (MTIs) were used. In Figure 9 the variation in A determined from the data that do not include the abnormal values and were binned into three-year MTIs is also shown, to indicate the difference between the yearly (*cf.* Figure 8(a)) and the three-year MTIs data. The equatorial-rotation rate determined from the Doppler-velocity data is shown for the three-year smoothed time series obtained from the annual values (*cf.* Figure 8(b)). As can be seen in Figure 9, the variation patterns in the equatorial-rotation rates derived from the sunspot-group data and the Doppler-velocity data closely resemble one another (correlation coefficient ≈ 0.5). In fact, during Cycle 23 the shapes of the curves are almost the same (the Doppler-velocity measurements are more accurate after 1995). This result indicates that the temporal variation in the equatorial-rotation rate determined from the Doppler-velocity measurements is of solar origin, which has been doubtful so far for the reason mentioned in Section 1. However, this result and conclusion is only suggestive and not compelling, because the uncertainties in A determined from the sunspot-group data that included the abnormal angular motions of the sunspot groups are large (in the figure the error bar represents one standard error level; the corresponding σ is very high). In addition, the abnormal angular motions of the sunspot groups may not represent the angular motions of the surface plasma. These motions may be the abnormal proper motions of the sunspot groups that took place at the locations of eruptive solar phenomena such as flares. The Doppler-velocity measurements may also be contaminated with the contributions from these plasma motions (the spikes in the daily Mt. Wilson velocity data were removed. Further trimming will create more data gaps and make the data more unrealistic).

On the other hand, the mean values $14.09^\circ \pm 0.13^\circ$ and $14.21^\circ \pm 0.07^\circ\,\mathrm{day}^{-1}$ (see Figures 2 and 3) of the equatorial-rotation rates determined from the SOON and Greenwich daily sunspot-group data, respectively, which included the abnormal ω values are significantly (more than 2σ level) lower than the corresponding values $14.45^\circ \pm 0.008^\circ$ and $14.51^\circ \pm 0.004^\circ$ determined from the data that did not include the abnormal values. Overall, it seems that mean values determined from the SOON data that included the abnormal ω values is somewhat closer to the mean value ($14.07^\circ \pm 0.02^\circ\,\mathrm{day}^{-1}$) of the equatorial-rotation rate determined from the Doppler-velocity data. In Figure 10 (the histogram of the distribution of the abnormal angular velocity values) there is a suggestion that the peaks of the open circle-long dashed curve in Figure 9 included the majority of the abnormal velocity values (in the range $10^\circ - 20^\circ$) that are somewhat consistent with the rotation rate of the Sun. Therefore, the similarity in the variations of the Doppler-velocity data and the sunspot-group data that included the abnormal motions suggest that the former may be largely of solar origin and are not spurious. Nevertheless, the highly unrealistic latitudinal gradient of the rotation (see Figures 2 and 3) that is obtained from the sunspot-group data that included the abnormal ω-values may have a strong influence on the corresponding equatorial-rotation rate, making the latter unreliable. For this reason, and because of the wide range and the large uncertainties in annual mean values (including all errors of measurements both random and systematic), the reality and reliability of the variation in the sunspot-group data that included the abnormal motions is doubtful. Hence, the similarity in the solar-cycle variations in the Doppler-velocity data and the sunspot-group data that included the abnormal

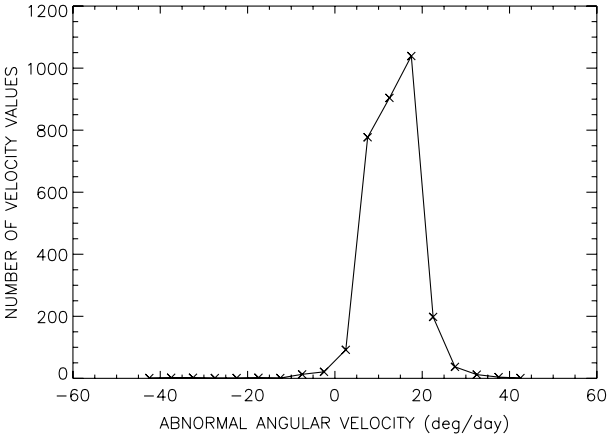

Figure 10 Distribution of the abnormal angular velocity values determined from the SOON sunspot-group data during the period 1 January 1977 to 31 January 2012

motions may instead suggest that the variation in the Doppler-velocity data (before 1995) could be contributed by the large uncertainties in this data.

As can be seen in Figure 8, the equatorial-rotation rate determined from the *Yohkoh*/SXT full-disk images for the period 1992 – 2001 by Chandra, Vats, and Iyer (2010) closely matches that determined from the sunspot-group data for all years except for the year 2000, where it has a high value. Close to this year there are humps in the variation of A determined from the sunspot group and the Doppler-velocity data as well, although they are small. Thus, the coronal rotation is strongly related to the angular motions of the surface magnetic features. (The phases of Ω_0 and A of the corona apparently agree even better, the agreement is particularly strong in minima.) However, the pattern of A determined from the SBCS seems to be considerably different from those of other data sets, particularly in the period 2001 – 2003. It even seems to be anti-correlated with that of the GONG data. The reason for this is not known. The similarity between the variation in the equatorial-rotation rate of sunspot groups and the corona and the variation in the internal equatorial-rotation rate is only in shape. The amplitude of the variation in the internal equatorial-rotation rate is very small.

4. Conclusions

The following conclusions can be drawn from our analysis:

i) A large portion (up to $\approx 30^\circ$ latitude) of the mean differential-rotation profile of the sunspot groups lies between those of the internal differential-rotation rates at $0.94R_\odot$ and $0.98R_\odot$. The portions up to 25° latitude on the mean profiles of the initial rotation rates of the up to eight days and longer than eight days living sunspot groups are close to those of the internal rotation near $0.96R_\odot$ and $0.8R_\odot$, respectively.

ii) At the end of Cycle 23 and at the beginning of Cycle 24, the value of the equatorial-rotation rate determined from the sunspot-group data is considerably higher than that at the beginning of Cycle 23. Overall, the variation pattern in the equatorial-rotation rate during Cycles 22 and 23 resembles the pattern of the known solar-cycle variation in the equatorial-rotation rate determined from sunspot data.

iii) There is a reasonable agreement between the variation pattern in the equatorial-rotation rate determined from the sunspot-group data and that determined from the GONG data [Ω_0]. Moreover, the variation in the internal equatorial-rotation rate apparently

leads the equatorial-rotation rate of sunspot groups by one to two years (the reason for this is not known to us).

iv) The pattern of the known solar-cycle variation in the equatorial-rotation rate of the solar corona determined from the *Yohkoh*/SXT full-disk images and SBCS closely matches that determined from the sunspot-group data (except during the period 2001 – 2003). This indicates that the coronal rotation is strongly related to the rotational motion of the surface magnetic features.

v) The variation in the equatorial-rotation rate determined from the Mount Wilson Doppler-velocity data substantially differs from the corresponding variation in the equatorial-rotation rate determined from the sunspot-group data without the values of the abnormal angular motions ($> |3^\circ|\,\mathrm{day}^{-1}$) of the sunspot groups, whereas it closely resembles the corresponding variation determined from the sunspot-group data with the values of the abnormal angular motions.

vi) Conclusion v) above may suggest that the solar-cycle variation in the surface equatorial-rotation rate determined from the Doppler-velocity measurements (before 1995) is caused by the inconsistency and uncertainties in the data (but this needs more studies to find a definite answer).

Acknowledgements The author thanks the anonymous referee for the detailed comments and useful suggestions, and H.M. Antia for providing the values of the internal-rotation rates that he has determined from GONG data. The author also thanks Luca Bertello for helpful comments and suggestions, B.A. Varghese for his help in making the figures, and the organizers of the LWS/SDO-3/SOHO26/GONG-2011 workshop for kindly providing a partial financial support to attend the workshop. This work used data obtained by the Global Oscillation Network Group (GONG) Program, managed by the National Solar Observatory (NSO), which is operated by AURA, Inc. under a cooperative agreement with the National Science Foundation. The data were acquired by instruments operated by the Big Bear Solar Observatory, High Altitude Observatory, Learmonth Solar Observatory, Udaipur Solar Observatory, Instituto de Astrofísico de Canarias, and Cerro Tololo Interamerican Observatory.

References

Antia, H.M., Basu, S., Chitre, S.M.: 2008, *Astrophys. J.* **681**, 680. doi:10.1086/588523.
Antia, H.M., Basu, S.: 2010, *Astrophys. J.* **720**, 494. doi:10.1088/0004-637X/720/1/494.
Babcock, H.W.: 1961, *Astrophys. J.* **133**, 572. doi:10.1086/147060.
Balthasar, H., Vázquez, M., Wöhl, H.: 1986, *Astron. Astrophys.* **155**, 87.
Brandenburg, A.: 2005, *Astrophys. J.* **625**, 539. doi:10.1086/429584.
Brajša, R., Ruždjak, D., Wöhl, H.: 2006, *Solar Phys.* **237**, 365. doi:10.1007/s11207-006-0076-7.
Carrington, R.C.: 1863 *Observations of the Spots on the Sun*, Williams and Norgate, London.
Chandra, S., Vats, H.O., Iyer, K.N.: 2010, *Mon. Not. Roy. Astron. Soc.* **407**, 1108. doi:10.1111/j.1365-2966.2010.16947.x.
Chou, D.-Y., Fisher, G.H.: 1989, *Astrophys. J.* **341**, 533. doi:10.1086/167514.
Dikpati, M., Gilman, P.A.: 2006, *Astrophys. J.* **649**, 498. doi:10.1086/506314.
D'Silva, S., Howard, R.F.: 1994, *Solar Phys.* **151**, 213. doi:10.1007/BF00679072.
Foukal, P.: 1972, *Astrophys. J.* **173**, 439. doi:10.1086/151435.
Godoli, G., Mazzucconi, F.: 1979, *Solar Phys.* **64**, 247. doi:10.1007/BF00151436.
Gough, D.O.: 2010, In: Hasan, S.S., Rutten, R.J. (eds.) *Magnetic Coupling Between the Interior and the Atmosphere of the Sun*, *Astrophys. Space Sci. Proc.* **SSA 1570-6591**, Springer, Berlin, 37. doi:10.1007/978-3-642-02859-5_4.
Gupta, S.S., Sivaraman, K.R., Howard, R.: 1999, *Solar Phys.* **188**, 225. doi:10.1023/A:1005229124554.
Hiremath, K.M.: 2002, *Astron. Astrophys.* **386**, 674. doi:10.1051/0004-6361:20020276.
Hiremath, K.M., Suryanarayana, G.S.: 2003, *Astron. Astrophys.* **411**, L497. doi:10.1051/0004-6361:20031618.
Howard, R., LaBonte, B.J.: 1980, *Astron. Astrophys.* **239**, L33. doi:10.1086/183286.
Howard, R., Gilman, P.I., Gilman, P.A.: 1984, *Astrophys. J.* **283**, 373. doi:10.1086/162315.

Howe, R., Christensen-Dalsgaard, J., Hill, F., Komm, R.W., Larsen, R.M., Schou, J., Thompson, M.J., Toomre, J.: 2000, *Astrophys. J. Lett.* **533**, L163. doi:10.1086/312623.
Javaraiah, J.: 2003a, *Solar Phys.* **212**, 23. doi:10.1023/A:1022912430585.
Javaraiah, J.: 2003b, In: Pevtsov, A.A., Uitenbroek, H. (eds.) *Current Theoretical Models and Future High Resolution Solar Observations: Preparing for ATST* **CS-286**, Astron. Soc. Pac., San Francisco, 325.
Javaraiah, J.: 2005, *Mon. Not. Roy. Astron. Soc.* **362**, 1311. doi:10.1111/j.1365-2966.2005.09403.x.
Javaraiah, J.: 2011, *Adv. Space Res.* **48**, 1032. doi:10.1016/j.asr.2011.05.004.
Javaraiah, J.: 2012, *Solar Phys.* **281**, 827. doi:10.1007/s11207-012-0106-6.
Javaraiah, J., Bertello, L., Ulrich, R.K.: 2005a, *Astrophys. J.* **626**, 579. doi:10.1086/429898.
Javaraiah, J., Bertello, L., Ulrich, R.K.: 2005b, *Solar Phys.* **232**, 25. doi:10.1007/s11207-005-8776-y.
Javaraiah, J., Gokhale, M.H.: 1995, *Solar Phys.* **158**, 173. doi:10.1007/BF00680841.
Javaraiah, J., Gokhale, M.H.: 1997a, *Solar Phys.* **170**, 389. doi:10.1023/A:1004928020737.
Javaraiah, J., Gokhale, M.H.: 1997b, *Astron. Astrophys.* **327**, 795.
Javaraiah, J., Gokhale, M.H.: 2002, *The Sun's Rotation*, Nova Science, New York.
Javaraiah, J., Komm, R.W.: 1999, *Solar Phys.* **184**, 41. doi:10.1023/A:1005028128077.
Javaraiah, J., Ulrich, R.K.: 2006, *Solar Phys.* **237**, 245. doi:10.1007/s11207-006-0130-5.
Javaraiah, J., Ulrich, R.K., Bertello, L., Boyden, J.E.: 2009, *Solar Phys.* **257**, 61. doi:10.1007/s11207-009-9342-9.
Jurdana-Šepić, R., Brajša, R., Wöhl, H., Hanslmeier, A., Poljančić, I., Svalgaard, L., Gissot, S.F.: 2011, *Astron. Astrophys.* **534**, A17. doi:10.1051/0004-6361/201014357.
Kambry, M.A., Nishikawa, J.: 1990, *Solar Phys.* **126**, 89. doi:10.1007/BF00158300.
Karak, B.B.: 2010, *Astrophys. J.* **724**, 1021. doi:10.1088/0004-637X/724/2/1021.
Kosovichev, A.G.: 2002, *Astron. Nachr.* **323**, 186. doi:10.1002/1521-3994(200208)323:3/4<186::AID-ASNA186>3.0.CO;2-I.
Kosovichev, A.G., Duvall, T.L. Jr., Scherrer, P.H.: 2000, *Solar Phys.* **192**, 159. doi:10.1023/A:1005251208431.
Meunier, N.: 2005, *Astron. Astrophys.* **436**, 1075. doi:10.1051/0004-6361:20042414.
Meyer, F., Schmidt, H.U., Simon, G.V., Weiss, N.O.: 1979, *Astron. Astrophys.* **76**, 35.
Moreno-Insertis, F.: 1986, *Astron. Astrophys.* **166**, 291.
Petrovay, K., Brown, J.C., van Driel-Gesztelyi, L., Fletcher, L., Marik, M., Stewart, G.: 1990, *Solar Phys.* **127**, 51. doi:10.1007/BF00158513.
Rosner, R., Weiss, N.O.: 1992, In: Harvey, K.L. (ed.) *The Solar Cycle* **CS-27**, Astron. Soc. Pac., San Francisco, 511.
Ruždjak, D., Ruždjak, V., Brajša, R., Wöhl, H.: 2004, *Solar Phys.* **221**, 225. doi:10.1023/B:SOLA.0000035066.96031.4f.
Schüssler, M., Rempel, M.: 2005, *Astron. Astrophys.* **441**, 337. doi:10.1051/0004-6361:20052962.
Shibata, K., Nozawa, R., Matsumoto, R., Sterling, A.C., Tajima, T.: 1990, *Astrophys. J.* **351**, L25. doi:10.1086/185671.
Sivaraman, K.R., Sivaraman, H., Gupta, S.S., Howard, R.: 2003, *Solar Phys.* **214**, 65. doi:10.1023/A:1024075100667.
Suryanarayana, G.S.: 2010, *New Astron.* **15**, 313. doi:10.1016/j.newast.2009.09.004.
Suzuki, M.: 2012, *Solar Phys.* **278**, 257. doi:10.1007/s11207-012-9946-3.
Tuominen, J.: 1962, *Z. Astrophys.* **55**, 110.
Tuominen, I., Virtanen, H.: 1988, *Adv. Space Res.* **8**, 141. doi:10.1016/0273-1177(88)90183-4.
Ulrich, R.K.: 2001, *Astrophys. J.* **560**, 466. doi:10.1086/322524.
Ulrich, R.K., Boyden, J.E.: 2005, *Astrophys. J. Lett.* **620**, L123. doi:10.1086/428724.
van Driel-Gesztelyi, L., Petrovay, K.: 1990, *Solar Phys.* **126**, 285. doi:10.1007/BF00153051.
Ward, F.: 1965, *Astrophys. J.* **141**, 534. doi:10.1086/148143.
Ward, F.: 1966, *Astrophys. J.* **145**, 416. doi:10.1086/148783.